

# Protein stoichiometry, structural plasticity and regulation of bacterial microcompartments

Lu-Ning Liu<sup>1,2</sup>, Mengru Yang<sup>2</sup>, Yaqi Sun<sup>2</sup> and Jing Yang<sup>2,3</sup>

Bacterial microcompartments (BMCs) are self-assembling prokaryotic organelles consisting of a polyhedral proteinaceous shell and encapsulated enzymes that are involved in CO<sub>2</sub> fixation or carbon catabolism. Addressing how the hundreds of building components self-assemble to form the metabolically functional organelles and how their structures and functions are modulated in the extremely dynamic bacterial cytoplasm is of importance for basic understanding of protein organelle formation and synthetic engineering of metabolic modules for biotechnological applications. Here, we highlight recent advances in understanding the protein composition and stoichiometry of BMCs, with a particular focus on carboxysomes and propanediol utilization microcompartments. We also discuss relevant research on the structural plasticity of native and engineered BMCs, and the physiological regulation of BMC assembly, function and positioning in native hosts.

## Addresses

<sup>1</sup> College of Marine Life Sciences and Frontiers Science Center for Deep Ocean Multispheres and Earth System, Ocean University of China, 266003 Qingdao, China

<sup>2</sup> Institute of Systems Molecular and Integrative Biology, University of Liverpool, Crown Street, Liverpool L69 7ZB, United Kingdom

<sup>3</sup> Materials Innovation Factory and Department of Chemistry, University of Liverpool, Liverpool L7 3NY, United Kingdom

Corresponding author: Liu, Lu-Ning ([luning.liu@liverpool.ac.uk](mailto:luning.liu@liverpool.ac.uk))

Current Opinion in Microbiology 2021, 62:133–141

This review comes from a themed issue on **Bacterial microcompartments**

Edited by **Warren Martin** and **Danielle Tullman-Ercek**

<https://doi.org/10.1016/j.mib.2021.07.006>

1369-5274/© 2021 The Author(s). Published by Elsevier Ltd. This is an open access article under the CC BY license (<http://creativecommons.org/licenses/by/4.0/>).

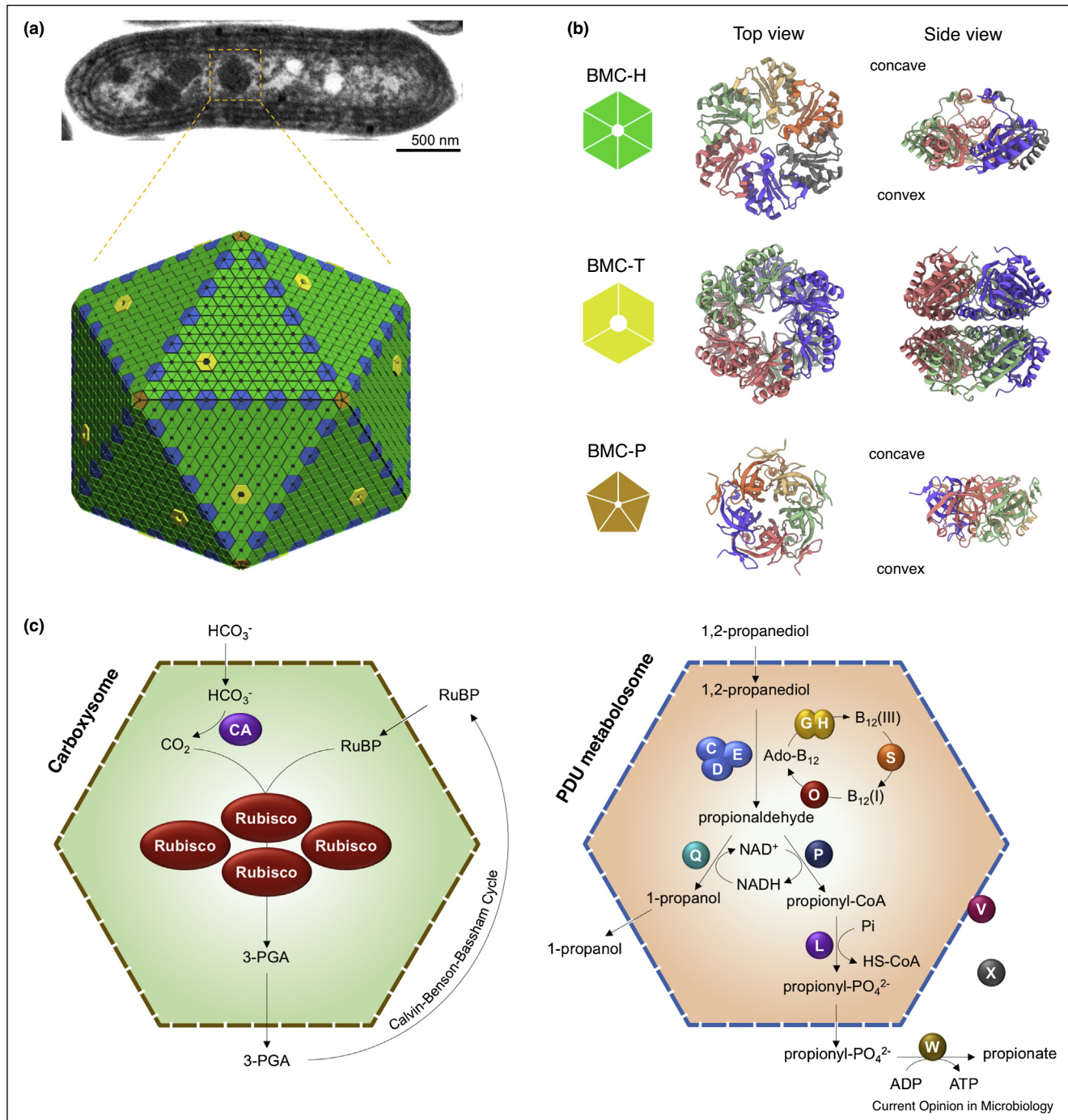
## Introduction

Intracellular compartmentalization and self-assembly of proteins into large supercomplex structures underpin most biological activities in living organisms. Bacterial microcompartments (BMCs) are a paradigm of proteinaceous compartmentalizing organelles widespread in prokaryotes [1] (Figure 1). These nanoscale organelles (typically 100–400 nm in size) sequester key metabolic pathways in the cytoplasm to enhance metabolic

performance. Bioinformatic analysis suggested that 23 types of BMC genetic operons or loci have been identified in up to 80% of the bacterial phyla [2]. An increasing number of new types of BMCs have been predicted in 45 phyla across diverse bacterial species [3]. All BMCs exhibit some common building principles: self-assembly, encapsulation, modularity, shell permeability, and structural plasticity.

- (1) Self-assembly: BMCs consist of thousands of protein peptides, which are highly efficient in recognizing and interacting with each other to form the megadalton-sized organelles.
- (2) Encapsulation: BMCs sequester multiple cargo enzymes that catalyze a series of biochemical reactions and toxic or volatile metabolic intermediates within an outer shell (Figure 1). This facilitates generation of a catalytically favorable microenvironment for the enclosed enzymes and pathways to enhance metabolism, enzyme stability and cooperation, and prevent unnecessary side reactions.
- (3) Modularity: The BMC loci comprise contiguous or dispersed clusters of genes required for BMC formation, function and regulation (Figure 2). These genes encode BMC shell components and cargo enzymes, as well as ancillary proteins for protein/complex assembly, metabolite transporters, regulatory proteins, and cytoskeletal proteins likely required for intracellular partitioning. The shell structure is generally conserved among distinct BMCs and is constructed of a series of homologous shell proteins (Figure 1). Shell proteins exist mainly in three forms: hexamers (BMC-H, containing one Pfam00936 domain) and pseudohexameric trimers (BMC-T, with two Pfam00936 domains) that tile the shell facets, and pentamers (BMC-P, with one Pfam03319 domain) that cap the vertices of the polyhedral shell [1,4]. A Bacterial Microcompartment Database, MCPdb (<https://mcpdb.mbi.ucla.edu/>), has recently been developed to facilitate searching the structures of BMC proteins and assemblies [5].
- (4) Shell permeability: The shell proteins are perforated by a central pore that varies in size, permitting selective passage of metabolites in and out of the BMC [6,7]. The concave side of shell proteins faces the cytoplasm and the convex side faces the BMC lumen [8] (Figure 1). These features are crucial for the shell semi-permeability to control the metabolic activities within the BMC.
- (5) Structural plasticity: The structural variations of BMCs and flexible protein–protein interactions

Figure 1



Overview of bacterial microcompartments (BMCs).

**(a)** Electron microscopy of a bacterial cell showing BMC polyhedrons (top) and a schematic model of the icosahedral BMC structure (bottom). **(b)** Models and structures of the BMC-H (CcmK2, PDB ID 2A1B), BMC-T (CcmP, PDB ID 5LSR), and BMC-P (CcmL, PDB ID 2QW7) proteins that are the building components of the BMC shell. **(c)** Schematic representation of the functions of two representative BMCs: the carboxysome (anabolic BMC) and PDU metabolosome (catabolic BMC). The BMC shell encases signature cargo enzymes and prevents the escape of  $\text{CO}_2$  or toxic propionaldehyde. Abbreviations: CA, carbonic anhydrase; 3-PGA, 3-phosphoglycerate; RuBP, ribulose 1,5-bisphosphate; Ado-B<sub>12</sub>, coenzyme B<sub>12</sub> or adenosylcobalamin; HS-CoA, coenzyme A; B<sub>12</sub>(I), cob(I)alamin; B<sub>12</sub>(III), cob(III)alamin; Pi, inorganic phosphate.

Figure 2

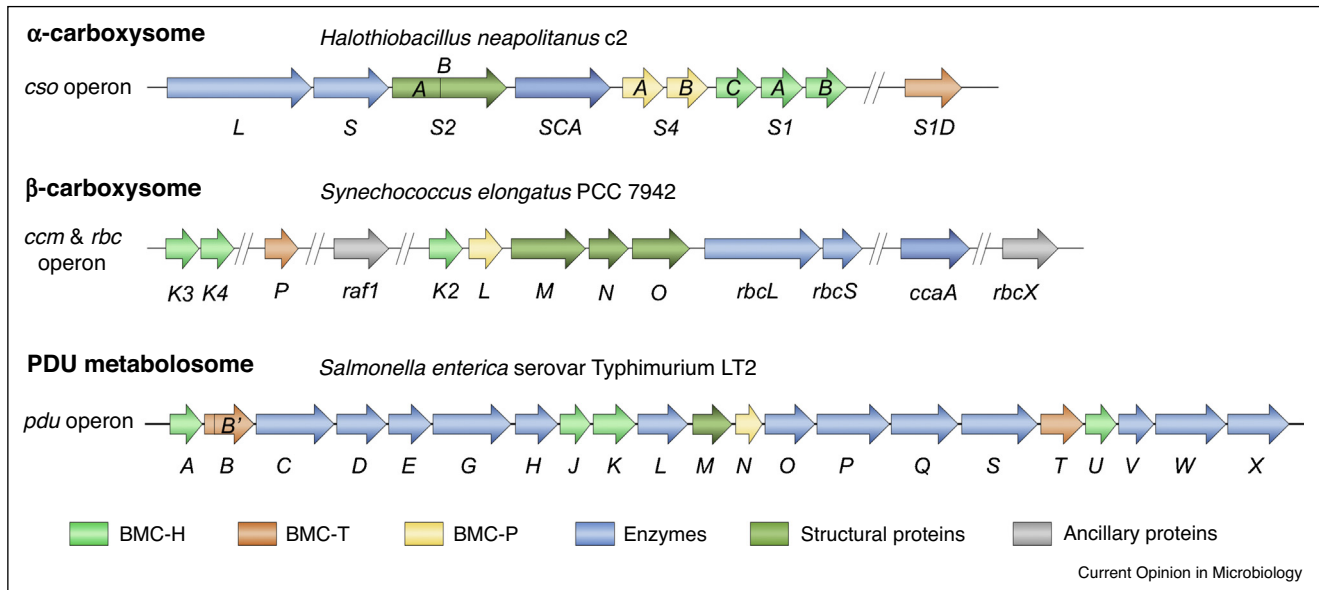


Diagram of the genomic organization of the  $\alpha$ -carboxysome and  $\beta$ -carboxysome and PDU metabolosome operons in representative bacterial species.

Genes encoding structurally and/or functionally similar proteins are presented in the same colors. Double-slash lines represent gaps between separated BMC operons.

may enable fine tuning of BMC assembly and shell permeability in response to a varying environment (see details below).

These structural and regulatory features provide the framework for the metabolic factories to play pivotal roles in autotrophic CO<sub>2</sub> fixation and catabolic processes and promoting bacterial fitness in specific environmental niches [9]. Moreover, they hold the promise for rationally repurposing BMC structures in various applications in synthetic biology [10,11], such as biofuel production [12<sup>\*\*</sup>,13].

According to their distinct functions, BMCs can be categorized into anabolic BMCs (carboxysomes) and catabolic BMCs (metabolosomes). The carboxysome is the central CO<sub>2</sub>-fixing organelle in all cyanobacteria and many chemolithotrophs. The metabolosomes degrade diverse carbon substrates in heterotrophs; the experimentally characterized metabolosomes include propanediol utilization (PDU), ethanolamine utilization (EUT), glyceryl radical enzyme-associated microcompartments (GRM), choline utilization (GRM2), fucose and rhamnose utilization (GRM5 and PVM), and 1-amino-2-propanol utilization (RMM) metabolosomes [14,15].

Recent technological advances in structural biology, microscopy, synthetic biology, proteomics, bioinformatics and computational modeling provide an unprecedented

opportunity to understand the assembly principles of BMCs [3,8,12<sup>\*\*</sup>,13,16,17,18<sup>\*</sup>,19<sup>\*</sup>,20,21<sup>\*\*</sup>,22<sup>\*\*</sup>,23<sup>\*\*</sup>,24<sup>\*\*</sup>]. In this review, we will focus on the recent advances in elucidating the composition, stoichiometry, structural plasticity and physiological regulation of BMCs, in particular the carboxysomes and PDU metabolosomes.

## Protein composition and stoichiometry of BMCs

### $\beta$ -carboxysome protein stoichiometry

The stoichiometric ratios of different building components and their interactions are key factors in driving the assembly and architecture of BMCs [17]. However, we still have limited knowledge about the actual protein composition and stoichiometry of BMCs. Cyanobacterial carboxysomes were the first discovered BMCs by electron microscopy (EM). Carboxysomes encapsulate carbonic anhydrase (CA) and the primary carboxylating enzymes, ribulose-1,5-bisphosphate carboxylase oxygenase (Rubisco). Bicarbonate (HCO<sub>3</sub><sup>-</sup>) in the cytosol can diffuse across the shell through the central pores of shell proteins, and is then converted to CO<sub>2</sub> by CA; the shell can prevent unwanted entry of O<sub>2</sub> and diminish CO<sub>2</sub> leakage into the cytosol. These mechanisms ensure the development of a CO<sub>2</sub>-rich and oxidizing microenvironment within the carboxysome to improve Rubisco carboxylation [25]. Recently, increasing efforts have focused on building carboxysomes in heterologous organisms to boost CO<sub>2</sub> fixation and cell growth [26,27,28<sup>\*\*</sup>,29].

Based on the forms of enclosed Rubisco, carboxysomes can be divided into two different classes:  $\alpha$ -carboxysomes and  $\beta$ -carboxysomes. The  $\beta$ -carboxysome of the rod-shaped cyanobacterium *Synechococcus elongatus* PCC7942 (Syn7942) has been extensively characterized. The Syn7942  $\beta$ -carboxysome shell is formed by BMC-H proteins (CcmK2, CcmK3, CcmK4) that tile the shell facets, the BMC-P protein CcmL that occupies the vertices of the polyhedron, and the BMC-T proteins (CcmO, CcmP). The core enzymes involve  $\beta$ -type CA (CcaA) and the key CO<sub>2</sub>-fixing enzyme Rubisco (comprising RbcL and RbcS, denoted as RbcL<sub>8</sub>S<sub>8</sub>) (Figure 1). Assembly of functional Rubisco and  $\beta$ -carboxysomes also requires ancillary proteins, such as Rubisco assembly factor 1 (Raf1) and RbcX [21<sup>\*\*</sup>,30].

To determine the exact stoichiometry of building components in the  $\beta$ -carboxysome, Sun *et al.* tagged a collection of carboxysome proteins (CcmK3, CcmK4, CcmL, CcmM, CcmN, RbcL, CcaA, RbcX) with fluorescent proteins, and then counted the copy numbers of these proteins in single  $\beta$ -carboxysomes by quantifying the discrete bleaching steps of tagged fluorescent proteins using single-molecule fluorescence microscopy [22<sup>\*\*</sup>]. The research revealed that the internal enzyme Rubisco is the most abundant component among all  $\beta$ -carboxysome proteins (853 copies, under moderate light, Table 1). The Rubisco content of the  $\beta$ -carboxysome is up to two folds greater than that of the  $\alpha$ -carboxysome [31], consistent with the highly dense packing of Rubisco within the  $\beta$ -carboxysome [32]. The second most abundant protein is CcmM (~700 per  $\beta$ -carboxysome), which serves as a linker protein binding Rubisco to the shell via the recruitment protein CcmN and induces phase separation into a liquid-like Rubisco matrix [19<sup>\*</sup>]. Protein quantification also offered the unique opportunity to evaluate the specific stoichiometric ratios of different carboxysome proteins, such as CcmK4 and CcmK3, which may be functionally correlated at the physiological context. Recently, CcmK4 and CcmK3 have been indicated to form heterohexamers with a 1:2 stoichiometry in the  $\beta$ -carboxysome [33<sup>\*</sup>].

### PDU metabolosome protein stoichiometry

The majority of BMCs are the metabolosomes that are found in a variety of bacteria and archaea including human gut microbes. The functionally distinct metabolosomes share universal biochemical reactions catalyzed by a signature enzyme, an aldehyde dehydrogenase, an alcohol dehydrogenase, and a phosphotransacylase. In the model pathogen *Salmonella enterica* serovar Typhimurium LT2 (*S. Typhimurium* LT2), the PDU metabolosome is constructed by 22 different types of proteins that are encoded by genes clustered in a single *pdu* operon (Figure 2). The core enzymes include diol dehydratase (PduCDE), phosphotransacylase (PduL), aldehyde dehydrogenase (PduP), alcohol dehydrogenase (PduQ), and

propionate kinase (PduW). The signature enzyme PduCDE catalyzes the conversion of 1,2-propanediol (1,2-PD) to propionaldehyde, which is then converted to propionyl coenzyme A (propionyl-CoA) or 1-propanol by PduP or PduQ, respectively. PduL catalyzes the conversion of propionyl-CoA to propionyl-phosphate, which is then converted into propionate by PduW to generate ATP. There are also other enzymes involved in the 1,2-PD metabolism, such as cobalamin reductase (PduS), adenosyltransferase (PduO), diol dehydratase reactivase (PduGH), and L-threonine kinase (PduX) for the reactivation of diol dehydratase and vitamin B<sub>12</sub> recycling.

To evaluate the accurate protein composition and stoichiometry of PDU metabolosomes, Yang *et al.* used mass spectrometry-based absolute quantification and a QconCAT (concatamer of standard peptides for absolute quantification) strategy to characterize the isolated PDU metabolosomes from *S. Typhimurium* LT2 [24<sup>\*\*</sup>]. Unlike the  $\beta$ -carboxysome in which the cargo enzyme Rubisco is the predominant component, the most abundant PDU element is the BMC-H shell protein PduJ, which accounts for over 44% of all PDU proteins (Table 1). This suggested a higher ratio of shell/cargo proteins and a relatively less crowded internal environment of PDU metabolosomes than those of the  $\beta$ -carboxysome [22<sup>\*\*</sup>]. As a comparison, in the PDU metabolosomes from *Citrobacter freundii*, PduB' appeared as the most abundant protein (31%) and PduJ only accounted for 18% of all PDU proteins [34]. This discrepancy probably implied the species-dependent variation of the PDU metabolosome protein stoichiometry. Protein quantification analysis also indicated the stoichiometric links of shell and cargo proteins, implicating their physiological coordination (Table 1). For example, the ratio of the trimeric shell protein PduB to the PduCDE dimer was roughly 1:1, and the ratio of the PduT trimer to the cargo PduS was 2:1. The physical associations of the minor proteins PduV, PduW and PduX with the PDU metabolosome were characterized using live-cell confocal imaging [24<sup>\*\*</sup>].

### Structural plasticity of BMCs

Unlike the robust and regular BMC structures that we used to think, more experimental results have shed light on the plasticity of natural BMC architectures. The biosynthesis and structures of  $\beta$ -carboxysomes in Syn7942 are highly regulated in response to environmental growth conditions. EM and fluorescence imaging showed that the size of  $\beta$ -carboxysomes and the abundance of individual proteins in the  $\beta$ -carboxysome could be adaptively modulated in response to changes in light intensities and CO<sub>2</sub> availabilities [22<sup>\*\*</sup>] (Figure 3, Table 1).

The BMC architectures are morphologically heterogeneous and vary in size and shape in their native hosts.

**Table 1****Protein composition and stoichiometry of the Syn7942  $\beta$ -carboxysome [22\*\*] and *S. Typhimurium* LT2 PDU metabolosome [24\*\*]**

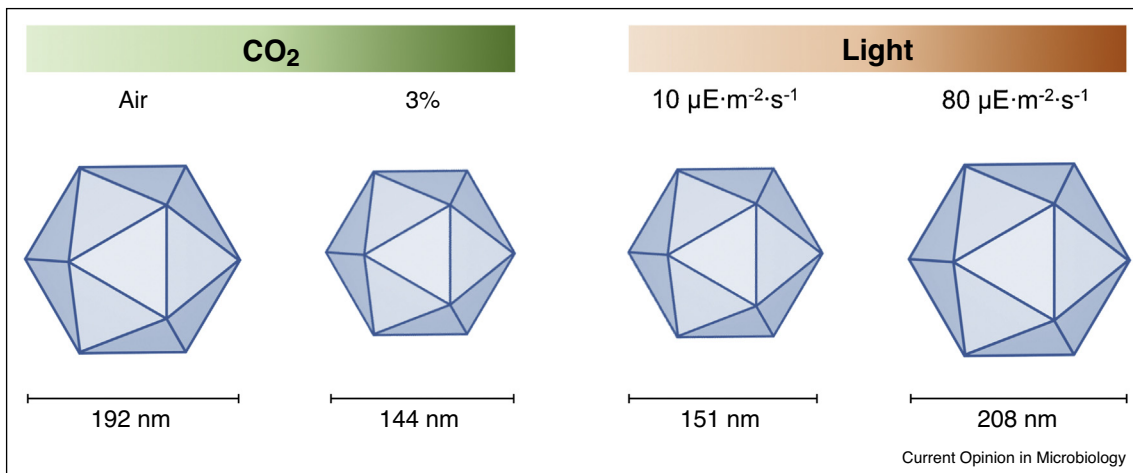
| $\beta$ -carboxysome |   |  |                                      |                      |               |                |
|----------------------|---|--|--------------------------------------|----------------------|---------------|----------------|
| Protein              | Description & function  | Structure                                  | Number of oligomers/monomers per BMC |                      |               |                |
|                      |   |  | Air/ML                               | CO <sub>2</sub> /ML  | LL            | HL             |
| CcmK3                | Minor shell proteins likely forming CcmK3/4 heterohexamers and CcmK4 homohexamer to tune shell permeability                       | BMC-H                                      | 15 $\pm$ 25                          | 29 $\pm$ 14          | 14 $\pm$ 5    | 14 $\pm$ 9     |
| CcmK4                |   | BMC-H                                      | 52 $\pm$ 32                          | 94 $\pm$ 44          | 52 $\pm$ 20   | 51 $\pm$ 16    |
| CcmL                 | Minor shell vertex protein, required for proper carboxysome assembly  | BMC-P                                      | 7.4 $\pm$ 3.4                        | 13.2 $\pm$ 4.8       | 6.8 $\pm$ 3.0 | 13.8 $\pm$ 4.8 |
| CcmM                 | Linker protein that induces Rubisco condensation, interacts with CcmN to the shell  | Monomer                                    | 719 $\pm$ 1433                       | 468 $\pm$ 425        | 483 $\pm$ 366 | 1176 $\pm$ 691 |
| CcmN                 | Structural protein, interact with CcmM and the shell proteins CcmK  | Monomer                                    | 74 $\pm$ 51                          | 52 $\pm$ 28          | 51 $\pm$ 20   | 82 $\pm$ 34    |
| Rubisco              | Key CO <sub>2</sub> -fixation enzyme  | RbcL <sub>8</sub> S <sub>8</sub>           | 853 $\pm$ 1150                       | 550 $\pm$ 832        | 367 $\pm$ 687 | 1507 $\pm$ 648 |
| CcaA                 | Carbonic anhydrase, encapsulated enzyme in carboxysomes for the conversion of HCO <sub>3</sub> <sup>-</sup> to CO <sub>2</sub>    | Hexamer                                    | 14 $\pm$ 14                          | 21 $\pm$ 14          | 11 $\pm$ 4    | 20 $\pm$ 10    |
| RbcX                 | Rubisco chaperone, required for proper carboxysome functions  | Dimer                                      | 20 $\pm$ 16                          | 19 $\pm$ 5           | 20 $\pm$ 5    | 20 $\pm$ 5     |
| PDU metabolosome     |   |  |                                      |                      |               |                |
| Protein              | Description & function  | Structure                                  | Number of oligomers/monomers per BMC |                      |               |                |
|                      |   |  | WT                                   | $\Delta$ <i>pduA</i> |               |                |
| PduA                 | Major shell protein, involved in selective molecular transport and interaction with PduP  | BMC-H                                      | 307 $\pm$ 17                         | 2 $\pm$ 0            |               |                |
| PduB                 | Major shell protein, involved in shell and cargo binding major shell protein, not essential for the assembly of PDU metabolosomes | BMC-T                                      | 224 $\pm$ 14                         | 52 $\pm$ 2           |               |                |
| PduB'                |   | BMC-T                                      | 278 $\pm$ 17                         | 52 $\pm$ 4           |               |                |
| PduJ                 | major shell protein, essential for the assembly and function of PDU metabolosomes, interact with PduP                             | BMC-H                                      | 869 $\pm$ 72                         | 1200 $\pm$ 148       |               |                |
| PduK                 | minor shell protein, involved in spatial organization of PDU metabolosomes  | BMC-H                                      | 86 $\pm$ 7                           | 97 $\pm$ 7           |               |                |
| PduM                 | Structural protein, essential for the assembly and function of PDU metabolosomes  | unknown                                    | 56 $\pm$ 9                           | 50 $\pm$ 7           |               |                |
| PduN                 | Minor shell protein, occupy the vertex of shell   | BMC-P                                      | 12 $\pm$ 1                           | 12 $\pm$ 2           |               |                |
| PduT                 | Minor shell protein, interact with PduS for electron transport  | BMC-T                                      | 96 $\pm$ 6                           | 92 $\pm$ 9           |               |                |
| PduU                 | Minor shell protein, not essential for the assembly and function of PDU metabolosomes   | BMC-H                                      | 22 $\pm$ 3                           | 18 $\pm$ 2           |               |                |
| PduC                 | Subunits of diol dehydratase, the N-terminus of PduD acts as an encapsulation peptide   | Dimer ( $\alpha\beta\gamma$ ) <sub>2</sub> | 272 $\pm$ 40                         | 126 $\pm$ 11         |               |                |
| PduD                 |   |  | 212 $\pm$ 23                         | 104 $\pm$ 12         |               |                |
| PduE                 |   |  | 188 $\pm$ 28                         | 102 $\pm$ 4          |               |                |
| PduG                 |   |  | 76 $\pm$ 9                           | 81 $\pm$ 10          |               |                |
| PduH                 | Subunits of diol dehydratase reactivase   | unknown                                    | 38 $\pm$ 4                           | 43 $\pm$ 4           |               |                |
| PduL                 | Phosphotransacylase, the N-terminal region acts as an encapsulation peptide   | Dimer                                      | 16 $\pm$ 1                           | 16 $\pm$ 2           |               |                |
| PduO                 | Adenosyltransferase   | unknown                                    | 146 $\pm$ 15                         | 118 $\pm$ 7          |               |                |
| PduP                 | Aldehyde dehydrogenase, the N-terminal region acts as an encapsulation peptide  | unknown                                    | 214 $\pm$ 31                         | 255 $\pm$ 29         |               |                |
| PduQ                 | Alcohol dehydrogenase   | unknown                                    | 145 $\pm$ 12                         | 114 $\pm$ 14         |               |                |
| PduS                 | Cobalamin reductase   | unknown                                    | 49 $\pm$ 4                           | 48 $\pm$ 6           |               |                |
| PduV                 | Sequence similar to Ras-like GTPase superfamily, connecting with filament-associated PDU metabolosome movement                    | unknown                                    | 7 $\pm$ 2                            | 6 $\pm$ 2            |               |                |

ML, moderate light; LL, low light; HL, high light [22\*\*]. The proteins with unknown structures are considered as monomers to show the stoichiometry.

Nanoindentation based on atomic force microscopy (AFM) demonstrated that the  $\beta$ -carboxysome architecture is mechanically softer than virus capsids, representing a mechanical signature of the BMC shells [32]. The absence of specific building components could also result in BMC structural remodeling, such as the elongated

BMCs when lacking BMC-P at the vertices [35,36]. In the PDU metabolosome, deleting the major shell protein PduA resulted in the altered abundance of shell proteins (such as the rising content of the shell protein PduJ) and internal enzymes, and thus the modified metabolic activities [24\*\*]. The results indicated the redundant roles of

Figure 3



Structural variations of  $\beta$ -carboxysomes in Syn7942 in response to changes in the CO<sub>2</sub> levels and light intensities during cell growth [22\*].

PduA and PduJ in retaining the assembly and overall architecture of PDU metabolosomes [37\*].

The structural plasticity of BMCs also occurred in specific protein–protein interactions. Experiments have suggested that disordered scaffolding proteins (CcmM35 in the  $\beta$ -carboxysome and CsoS2 in the  $\alpha$ -carboxysome) drive Rubisco coalescence in the cytoplasm via weak and transient multivalent interactions [18\*,19\*], promoting carboxysome assembly via liquid–liquid phase separation. Additionally, BMCs contain several paralogs of shell proteins that are structurally and functionally correlated to each other. It was proposed that CcmK3 and CcmK4 of Syn7942 could form heterohexamers in a pH-dependent manner, with a 2:4 stoichiometry [33\*]. Similar CcmK3–CcmK4 heterohexamers were suggested to exist in the *Synechocystis* sp. PCC 6803  $\beta$ -carboxysomes [38], implying a general principle that may alter the  $\beta$ -carboxysome shell structure and permeability. Another fashion to tune the molecule passage across the shell has been proposed by the dynamic ‘capping’ of BMC-P and BMC-H shell proteins in the BMC shells [33\*,39]. Consistently, high-speed AFM has visualized the dynamic self-assembly and protein–protein interactions of BMC shell proteins [40], and has revealed that the self-assembly dynamics of shell facets is sensitive to environmental changes [41]. Although we still do not fully understand the underlying molecular mechanisms, these assembly and modular properties may play roles in the intrinsic regulations of shell assembly and permeability and the structural remodeling of BMCs at multiple levels.

In the context of reconstituted shells, both large  $\alpha$ -carboxysome shells ( $\sim$ 100 nm in diameter) [12\*] and *Klebsiella pneumoniae* GRM2 BMC minishells expressed in *Escherichia coli* exhibited marked structural variations

[42,43\*]. Characterization of the reconstituted *Haliangium ochraceum* BMC shells of  $\sim$ 40 nm in diameter identified the structural plasticity of protein–protein interactions, which are subject to the local and global structural variations of the synthetic shells [44\*]. The structural flexibility of shell structures has important implications on the variations of native BMC structures and the tuning mechanism of shell permeability.

### Regulation of BMC biosynthesis and intracellular positioning

BMC biosynthesis, structure and function are physiologically integrated into the metabolic and regulatory networks of native host cells. Live-cell fluorescent imaging revealed that the increase in light intensity during cell growth could stimulate the biosynthesis of carboxysomes, represented by the increased numbers of carboxysomes per cell, and the enhanced carboxysomes CO<sub>2</sub>-fixing activities [45]. This regulation is closely correlated with the redox states of the photosynthetic electron transport chain. The intracellular localization and CO<sub>2</sub>-fixing activities of  $\beta$ -carboxysomes in Syn7942 cells were further demonstrated to be actively modulated under diurnal light-dark cycles that mimicked the natural growth conditions of cyanobacterial cells [46]. Deletion of the circadian clock protein KaiA altered the number of carboxysomes per cell and carboxysome localization, highlighting the role of the circadian clock in governing carboxysome biosynthesis and positioning in cyanobacteria [46].

The intracellular spatial positioning and regulation of carboxysomes are crucial for cell metabolism and growth. It was proposed that the cell poles play important roles in  $\beta$ -carboxysome and degradation of inactive or damaged  $\beta$ -carboxysomes in cyanobacteria [23\*,47]. Moreover, equal segregation of  $\beta$ -carboxysomes between daughter

cells is required to retain carboxysome inheritance during cell division [48]. The specific localization of carboxysomes within cyanobacterial cells was suggested to be mediated by interactions with cytoskeleton components such as ParA [48] (also termed McdA [49]). Recently, a McdAB system was identified to determine  $\beta$ -carboxysome partitioning in Syn7942, through the interactions of McdB with both carboxysomes and McdA [49]. It was further indicated that the McdAB systems exist among  $\beta$ -cyanobacteria that possess  $\beta$ -carboxysomes [50]. Recently, the McdAB-like system has also been identified in  $\alpha$ -carboxysome-containing proteobacteria, suggesting a common mechanism underlying the *in vivo* positioning of both  $\alpha$ -carboxysomes and  $\beta$ -carboxysomes [51]. This mechanism might be extendable to the sub-cellular positioning of other BMCs across the bacterial kingdom.

## Conclusions

The natural self-assembling features of BMCs and their significance in metabolic enhancement have attracted increasing interest in fundamental understanding of protein self-assembly and repurposing BMC structures for diverse biotechnological purposes. Advanced understanding of BMC protein stoichiometry, structural plasticity and regulation spotlighted the variations and tunability of native BMC structure and function, and the prospects for rational design and reprogramming of BMCs for specific functions in a controllable manner. It would be interesting to explore the diverse mechanisms that govern the functional stoichiometry and assembly of different types of BMCs. In addition, understanding the protein composition and the roles of individual components of BMCs has fostered synthetic engineering of BMCs and shell structures with the ‘minimal’ composition [8,27,43<sup>\*\*</sup>,44<sup>\*\*</sup>,52<sup>\*</sup>]. Future efforts can focus on how to select the minimal required building components and encapsulation strategies and how to adjust the stoichiometric ratios of distinct components and protein–protein interactions, to obtain specific BMC structures, efficient cargo encapsulation and programmable shell permeability. To manipulate the functional performance of engineered BMC structures, we also need to consider how to ensure their functional integrity in the metabolic and regulatory networks of the heterologous hosts. This may involve genetic engineering and modulation of necessary auxiliary proteins, regulatory factors and other cellular components.

## Conflict of interest statement

Nothing declared.

## Acknowledgements

This work was supported by the National Natural Science Foundation of China (32070109), the Royal Society (URFR180030, RGFEA181061, RGFEA180233), the Biotechnology and Biological Sciences Research Council (BBSRC) (BB/V009729/1, BB/M024202/1, BB/R003890/1).

## References and recommended reading

Papers of particular interest, published within the period of review, have been highlighted as:

- of special interest
  - of outstanding interest
1. Kerfeld CA, Aussignargues C, Zarzycki J, Cai F, Sutter M: **Bacterial microcompartments**. *Nat Rev Microbiol* 2018, **16**:277–290.
  2. Axen SD, Erbilgin O, Kerfeld CA: **A taxonomy of bacterial microcompartment loci constructed by a novel scoring method**. *PLoS Comput Biol* 2014, **10**:e1003898.
  3. Sutter M, Melnicki MR, Schulz F, Woyke T, Kerfeld CA: **A catalog of the diversity and ubiquity of bacterial microcompartments**. *Nat Commun* 2021, **12**:3809 <http://dx.doi.org/10.1038/s41467-021-24126-4>.
  4. Kerfeld CA, Erbilgin O: **Bacterial microcompartments and the modular construction of microbial metabolism**. *Trends Microbiol* 2015, **23**:22–34.
  5. Ochoa JM, Bair K, Holton T, Bobik TA, Yeates TO: **MCPdb: the bacterial microcompartment database**. *PLoS One* 2021, **16**:e0248269.
  6. Faulkner M, Szabó I, Weetman SL, Sicard F, Huber RG, Bond PJ, Rosta E, Liu LN: **Molecular simulations unravel the molecular principles that mediate selective permeability of carboxysome shell protein**. *Sci Rep* 2020, **10**:17501
  - Computational simulations and genetic modification revealed the semi-permeability of the  $\beta$ -carboxysome major shell protein CcmK2 to control passage of the reactants and products for Rubisco-catalyzed CO<sub>2</sub> fixation.
  7. Mahinthichaichan P, Morris DM, Wang Y, Jensen GJ, Tajkhorshid E: **Selective permeability of carboxysome shell pores to anionic molecules**. *J Phys Chem B* 2018, **122**:9110–9118
  - *In silico* investigation on the permeability of the shell proteins CsoS1A of the  $\alpha$ -carboxysome and CcmK4 of the  $\beta$ -carboxysome.
  8. Sutter M, Greber B, Aussignargues C, Kerfeld CA: **Assembly principles and structure of a 6.5-MDa bacterial microcompartment shell**. *Science* 2017, **356**:1293–1297.
  9. Stewart AM, Stewart KL, Yeates TO, Bobik TA: **Advances in the world of bacterial microcompartments**. *Trends Biochem Sci* 2021, **46**:406–416 <http://dx.doi.org/10.1016/j.tibs.2020.12.002>.
  10. Planamente S, Frank S: **Bio-engineering of bacterial microcompartments: a mini review**. *Biochem Soc Trans* 2019, **47**:765–777.
  11. Lee MJ, Palmer DJ, Warren MJ: **Biotechnological advances in bacterial microcompartment technology**. *Trends Biotechnol* 2019, **37**:325–336.
  12. Li T, Jiang Q, Huang J, Aitchison CM, Huang F, Yang M, Dykes GF, He H-L, Wang Q, Sprick RS *et al.*: **Reprogramming bacterial protein organelles as a nanoreactor for hydrogen production**. *Nat Commun* 2020, **11**:5448
  - The study showed the first synthetically engineered near native carboxysome shell and demonstrated its potential as a robust nano-bioreactor to encapsulate hydrogenases for improving H<sub>2</sub> production. It also indicated the O<sub>2</sub>-limited interior environment created by the carboxysome shell, which could facilitate the catalytic activities of oxygen-sensitive enzymes.
  13. Lee MJ, Mantell J, Hodgson L, Alibhai D, Fletcher JM, Brown IR, Frank S, Xue WF, Verkade P, Woolfson DN *et al.*: **Engineered synthetic scaffolds for organizing proteins within the bacterial cytoplasm**. *Nat Chem Biol* 2018, **14**:142–147.
  14. Stewart KL, Stewart AM, Bobik TA: **Prokaryotic organelles: bacterial microcompartments in *E. coli* and *Salmonella***. *EcoSal Plus* 2020, **9** <http://dx.doi.org/10.1128/ecosalplus.ESP-0025-2019>.
  15. Liu LN: **Bacterial metabolosomes: new insights into their structure and bioengineering**. *Microbial Biotechnol* 2021, **14**:88–93.

16. Mohajerani F, Sayer E, Neil C, Inlow K, Hagan MF: **Mechanisms of scaffold-mediated microcompartment assembly and size control.** *ACS Nano* 2021, **15**:4197-4212.
17. Li Y, Kennedy NW, Li S, Mills CE, Tullman-Ercek D, de la Cruz MO: **Computational and experimental approaches to controlling bacterial microcompartment assembly.** *ACS Cent Sci* 2021, **7**:658-670 <http://dx.doi.org/10.1101/2021.01.18.427120>.
18. Oltrogge LM, Chaijarasphong T, Chen AW, Bolin ER, Marqusee S, Savage DF: **Multivalent interactions between CsoS2 and Rubisco mediate alpha-carboxysome formation.** *Nat Struct Mol Biol* 2020, **27**:281-287
- In the  $\alpha$ -carboxysome, the N-terminus of CsoS2 binds with Rubisco via weak multivalent interactions, facilitating  $\alpha$ -carboxysome cargo encapsulation and Rubisco condensation.
19. Wang H, Yan X, Aigner H, Bracher A, Nguyen ND, Hee WY, Long BM, Price GD, Hartl FU, Hayer-Hartl M: **Rubisco condensate formation by CcmM in beta-carboxysome biogenesis.** *Nature* 2019, **566**:131-135
- The structural protein CcmM was shown to interact with Rubisco without replacing RbcS, and induce formation of a liquid-like Rubisco matrix to promote  $\beta$ -carboxysome assembly.
20. Lee MJ, Mantell J, Brown IR, Fletcher JM, Verkade P, Pickersgill RW, Woolfson DN, Frank S, Warren MJ: **De novo targeting to the cytoplasmic and luminal side of bacterial microcompartments.** *Nat Commun* 2018, **9**:3413.
21. Huang F, Kong W, Sun Y, Chen T, Dykes GF, Jiang YL, Liu LN: **Rubisco accumulation factor 1 (Raf1) plays essential roles in mediating Rubisco assembly and carboxysome biogenesis.** *Proc Natl Acad Sci U S A* 2020, **117**:17418-17428
- The research applied biochemical and *in vivo* physiological assays and cryo-EM to study how the Rubisco assembly factor Raf1 binds with Rubisco and how Raf1 mediates Rubisco assembly and  $\beta$ -carboxysome formation. The study led to a new proposed model of  $\beta$ -carboxysome assembly.
22. Sun Y, Wollman AJM, Huang F, Leake MC, Liu LN: **Single-organelle quantification reveals the stoichiometric and structural variability of carboxysomes dependent on the environment.** *Plant Cell* 2019, **31**:1648-1664
- By exploiting advanced microscopic imaging, the research characterized the physiological protein stoichiometry of in the context of single  $\beta$ -carboxysome. The study also showed the protein stoichiometry and structure of  $\beta$ -carboxysomes are modular to the changing environment during cell growth.
23. Hill NC, Tay JW, Altus S, Bortz DM, Cameron JC: **Life cycle of a cyanobacterial carboxysome.** *Sci Adv* 2020, **6**:eaba1269
- Based on advanced live-cell fluorescence imaging, this study characterized the  $\beta$ -carboxysome content, localization and activities during cell growth and division, outlining the biogenesis and degrading processes of  $\beta$ -carboxysomes in *Synechococcus* sp. PCC 7002.
24. Yang M, Simpson DM, Wenner N, Brownridge P, Harman VM, Hinton JCD, Beynon RJ, Liu LN: **Decoding the stoichiometric composition and organisation of bacterial metabolosomes.** *Nat Commun* 2020, **11**:1976
- The first study using absolute protein quantification to characterize the stoichiometric and structural signatures of native PDU metabolosomes from *Salmonella enterica* serovar Typhimurium LT2 and the stoichiometric plasticity of PDU metabolosomes when lacking the major shell protein PduA.
25. Chen AH, Robinson-Mosher A, Savage DF, Silver PA, Polka JK: **The bacterial carbon-fixing organelle is formed by shell envelopment of preassembled cargo.** *PLoS One* 2013, **8**:e76127.
26. Fang Y, Huang F, Faulkner M, Jiang Q, Dykes GF, Yang M, Liu LN: **Engineering and modulating functional cyanobacterial CO<sub>2</sub>-fixing organelles.** *Front Plant Sci* 2018, **9**:739.
27. Long BM, Hee WY, Sharwood RE, Rae BD, Kaines S, Lim Y-L, Nguyen ND, Massey B, Bala S, von Caemmerer S *et al.*: **Carboxysome encapsulation of the CO<sub>2</sub>-fixing enzyme Rubisco in tobacco chloroplasts.** *Nat Commun* 2018, **9**:3570.
28. Flamholz AI, Dugan E, Blikstad C, Gleizer S, Ben-Nissan R, Amram S, Antonovsky N, Ravishanker S, Noor E, Bar-Even A *et al.*: **Functional reconstitution of a bacterial CO<sub>2</sub> concentrating mechanism in Escherichia coli.** *eLife* 2020, **9**:e59882
- The study showed the successful reconstitution of a CO<sub>2</sub>-concentrating mechanism including  $\alpha$ -carboxysomes and bicarbonate transporters into *E. coli*. By adjusting the protein expression levels through natural selection, the engineering *E. coli* strain could grow at ambient CO<sub>2</sub> levels.
29. Hennacy JH, Jonikas MC: **Prospects for engineering biophysical CO<sub>2</sub> concentrating mechanisms into land plants to enhance yields.** *Annu Rev Plant Biol* 2020, **71**:461-485.
30. Huang F, Vasieva O, Sun Y, Faulkner M, Dykes GF, Zhao Z, Liu LN: **Roles of RbcX in carboxysome biosynthesis in the cyanobacterium Synechococcus elongatus PCC7942.** *Plant Physiol* 2019, **179**:184-194.
31. Iancu CV, Ding HJ, Morris DM, Dias DP, Gonzales AD, Martino A, Jensen GJ: **The structure of isolated Synechococcus strain WH8102 carboxysomes as revealed by electron cryotomography.** *J Mol Biol* 2007, **372**:764-773.
32. Faulkner M, Rodriguez-Ramos J, Dykes GF, Owen SV, Casella S, Simpson DM, Beynon RJ, Liu LN: **Direct characterization of the native structure and mechanics of cyanobacterial carboxysomes.** *Nanoscale* 2017, **9**:10662-10673.
33. Sommer M, Sutter M, Gupta S, Kirst H, Turmo A, Lechno-Yossef S, Burton RL, Saechao C, Sloan NB, Cheng X *et al.*: **Heterohexamers formed by CcmK3 and CcmK4 increase the complexity of beta carboxysome shells.** *Plant Physiol* 2019, **179**:156-167
- The first study showing the presence of the heterohexamer shell protein formed by CcmK3 and CcmK4 and suggesting the role of CcmK3-CcmK4 heterohexamers in tuning shell permeability and assembly.
34. Mayer MJ, Juodeikis R, Brown IR, Frank S, Palmer DJ, Deery E, Beal DM, Xue W-F, Warren MJ: **Effect of bio-engineering on size, shape, composition and rigidity of bacterial microcompartments.** *Sci Rep* 2016, **6**:36899.
35. Sutter M, Wilson SC, Deutsch S, Kerfeld CA: **Two new high-resolution crystal structures of carboxysome pentamer proteins reveal high structural conservation of CcmL orthologs among distantly related cyanobacterial species.** *Photosynth Res* 2013, **118**:9-16.
36. Cheng S, Sinha S, Fan C, Liu Y, Bobik TA: **Genetic analysis of the protein shell of the microcompartments involved in coenzyme B12-dependent 1, 2-propanediol degradation by Salmonella.** *J Bacteriol* 2011, **193**:1385-1392.
37. Kennedy NW, Ikonomova SP, Slininger Lee M, Raeder HW, Tullman-Ercek D: **Self-assembling shell proteins pdua and pduj have essential and redundant roles in bacterial microcompartment assembly.** *J Mol Biol* 2021, **433**:166721
- The study showed that the major shell proteins PduA and PduJ have the redundant roles in PDU microcompartment assembly.
38. Garcia-Alles LF, Root K, Maveyraud L, Aubry N, Lesniewska E, Mourey L, Zenobi R, Truan G: **Occurrence and stability of hetero-hexamer associations formed by beta-carboxysome CcmK shell components.** *PLoS One* 2019, **14**:e0223877.
39. Hagen A, Sutter M, Sloan N, Kerfeld CA: **Programmed loading and rapid purification of engineered bacterial microcompartment shells.** *Nat Commun* 2018, **9**:2881.
40. Sutter M, Faulkner M, Aussignargues C, Paasch BC, Barrett S, Kerfeld CA, Liu LN: **Visualization of bacterial microcompartment facet assembly using high-speed atomic force microscopy.** *Nano Lett* 2016, **16**:1590-1595.
41. Faulkner M, Zhao LS, Barrett S, Liu LN: **Self-assembly stability and variability of bacterial microcompartment shell proteins in response to the environmental change.** *Nanoscale Res Lett* 2019, **14**:54.
42. Cesle EE, Filimonenko A, Tars K, Kalnins G: **Variety of size and form of GRM2 bacterial microcompartment particles.** *Protein Sci* 2021, **30**:1035-1043 <http://dx.doi.org/10.1002/pro.4069>.
43. Kalnins G, Cesle EE, Jansons J, Liepins J, Filimonenko A, Tars K: **Encapsulation mechanisms and structural studies of GRM2 bacterial microcompartment particles.** *Nat Commun* 2020, **11**:388
- The study showed the first recombinant GRM2 minishell and cryo-EM analysis revealed the variability of GRM2 minishell architectures.

44. Greber BJ, Sutter M, Kerfeld CA: **The plasticity of molecular interactions governs bacterial microcompartment shell assembly.** *Structure* 2019, **27**:749-763  
Cryo-EM analysis of the synthetic *H. ochraceum* BMC minishells illustrated a remarkable degree of the plasticity of local protein-protein interactions within the minishells and the global shell structures.
45. Sun Y, Casella S, Fang Y, Huang F, Faulkner M, Barrett S, Liu LN: **Light modulates the biosynthesis and organization of cyanobacterial carbon fixation machinery through photosynthetic electron flow.** *Plant Physiol* 2016, **171**:530-541.
46. Sun Y, Huang F, Dykes GF, Liu LN: **Diurnal regulation of *in vivo* localization and CO<sub>2</sub>-fixing activity of carboxysomes in *Synechococcus elongatus* PCC 7942.** *Life (Basel)* 2020, **10**:169.
47. Cameron JC, Wilson SC, Bernstein SL, Kerfeld CA: **Biogenesis of a bacterial organelle: the carboxysome assembly pathway.** *Cell* 2013, **155**:1131-1140.
48. Savage DF, Afonso B, Chen AH, Silver PA: **Spatially ordered dynamics of the bacterial carbon fixation machinery.** *Science* 2010, **327**:1258-1261.
49. MacCready JS, Hakim P, Young EJ, Hu L, Liu J, Osteryoung KW, Vecchiarelli AG, Ducat DC: **Protein gradients on the nucleoid position the carbon-fixing organelles of cyanobacteria.** *eLife* 2018, **7**:e39723.
50. MacCready JS, Basalla JL, Vecchiarelli AG: **Origin and evolution of carboxysome positioning systems in cyanobacteria.** *Mol Biol Evol* 2020, **37**:1434-1451.
51. MacCready JS, Tran L, Basalla JL, Hakim P, Vecchiarelli AG: **The McdAB system positions  $\alpha$ -carboxysomes in proteobacteria.** *Mol Microbiol* 2021, **00**:1-21.
52. Sutter M, Laughlin TG, Sloan NB, Serwas D, Davies KM, Kerfeld CA: **Structure of a synthetic  $\beta$ -carboxysome shell.** *Plant Physiol* 2019, **181**:1050-1058  
Cryo-EM structural analysis of the recombinant  $\beta$ -carboxysome minishells consisting of CcmK1, CcmK2, CcmO and CcmL.